

## THE RICE DISTRIBUTION AND ML POSITIONING USING RECEIVED SIGNAL POWERS IN SENSOR NETWORKS

MAKOTO TANIKAWARA, KENGO OHBA, YUKIHIRO KUBO AND SUEO SUGIMOTO

Department of Electrical and Electronic Engineering  
Ritsumeikan University  
Noji-Higashi, Kusatsu City, Shiga 525-8577, Japan  
re008993@ed.ritsumei.ac.jp

Received March 2011; revised July 2011

**ABSTRACT.** *In this paper, we present statistical models based on the Rice distribution and ML (maximum likelihood) positioning algorithms for received signal powers in sensor networks. The purpose of this study is to develop the indoor positioning system with utilizing the IEEE Std 802.15.4 [1] based the wireless sensor network. We estimate the position of nodes (active tags) in sensor networks. Reference nodes (base stations) exist with known coordinates, typically because they are part of an installed infrastructure. Other nodes are blind nodes, whose coordinates need to be estimated. These blind nodes are often mobile and attached to assets that need to be tracked. The variation of the RSSI is large because of the influence by the measurement environment. Therefore, it is necessary to acquire a lot of the RSSI (Received Signal Strength Indicator) data to improve the position estimation. In this paper, we present the models of RSSI of radio signal propagation applying the Rice distribution, in the special occasion, including the Rayleigh and gamma distributions. We propose a positioning algorithm based on the ML method from the probability density functions of the signal powers.*

**Keywords:** Indoor positioning, Received signal strength, Rice distribution, Sensor network

**1. Introduction.** Wireless sensor networks can supply sensing data to applications that adapt to the user's circumstances in a ubiquitous computing environment. Their systems are applied in a variety of fields, such as commodities management, energy monitoring, and a wireless attraction system. Thus, position information is very important in sensor networks.

Therefore, sensor nodes send sensing data to a base station for data collection. If they are appropriately designed, sensor nodes can work autonomously to measure temperature, humidity, acceleration, and so on. In addition, sensor locations are important too, because sensing data are meaningless if the sensor location is unknown in various applications.

The most popular method to acquire position information is GPS (Global Positioning System). GPS provides highly accurate position and velocity. The main factor limiting the use of GPS is the requirement for line-of-sight between the receiver antenna and the satellites. Therefore, methods of the indoor measurement applying GPS, pseudolite method and IMES (Indoor Messaging System) are proposed [2, 3]. However, positioning of pseudolite method is difficult due to multipath signals and cycle slips in indoor environment. Furthermore, the cost of the infrastructure maintenance rises because a tightly-synchronized signal is necessary. On the other hand, IMES method is constructed by using the same frequency of the GPS signal and the modulation method. It is expected as a technique of a seamless measurement using GPS though there are problems of the measurement time and the operation method, etc.

As alternative to GPS, some methods to acquire position information without GPS have been studied [4, 5, 6]. Consequently, in indoor positioning an Inertial Navigation System (INS) provides position, velocity and attitude autonomously at a rate of several tens of Hz. However, its errors are accumulated owing to drift of IMU (Inertial Measurement Unit) [7, 8].

The positioning method uses wireless communication, especially, methods using radio property such as received signal power, time of arrival (TOA), directional antenna (Cell-ID) and angle of arrival (AOA).

In this paper, a location estimation method which utilizes the RSSI (Received Signal Strength Indicator) obtained as a by-product of the data communication between nodes for wireless sensor networks is focused on. However, the RSSI has a larger variation because it is subject to the effects of fading or shadowing. Thus we propose the ML based distance estimation method that can take into account the radio environment. First, in Section 2, we introduce the specification and functions of a ubiquitous device which is applied in this paper. Next, in Section 3, we present the statistical models of RSSI of radio propagation based on the Rice distribution [9, 10] and the ML methods of estimating the parameters in these models derived from the Rice distribution. Furthermore, based on these statistical models of RSSI, ML algorithms are derived for estimating locations of tags. The fitness test for the many statistical models of RSSI is derived based on AIC (Akaike's Information Criterion) [11, 12]. Also we show the experimental results for the model determination of RSSI and the location estimation of tags based on our derived methods. Finally, in Section 6, we conclude the paper.

**2. System Equipments.** In this paper, we construct a system to use the following equipment.

**2.1. IEEE STD 802.15.4.** IEEE Std 802.15.4 has three frequency bands: 868 MHz (868-868.6 MHz), 915 MHz (902-928 MHz) and 2.4 GHz (2.4-2.4835 GHz) bands; however, only the 2.4 GHz band is allowed in Japan. The bit rate, symbol rate and modulation are 250 kbits/sec, 62.5 ksymbols/sec and offset-quadrature phase shift keying (O-QPSK), respectively. The 2.4 GHz band is included in industrial, scientific and medical (ISM) band, so it is rich in interference. To mitigate the interference, therefore, direct sequence spread spectrum (DS-SS) with processing gain of 8 is adopted in the standard. The chip rate is 2 Mchips/sec.

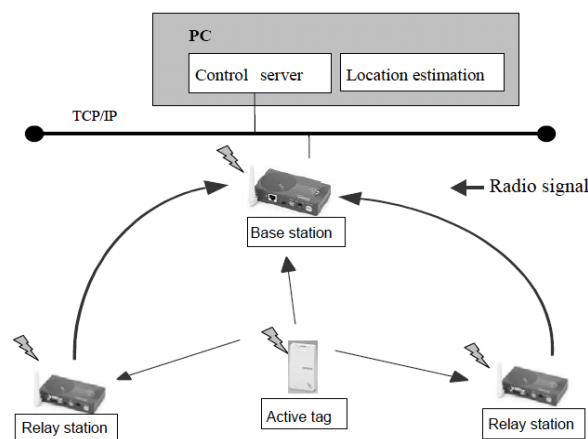


FIGURE 1. Description of the system

We implemented our techniques in Ubiquitous Device the “smartMODULE”, which is a sensor network developed by Hitachi Industrial Equipment System Co. Ltd., Japan. The “smartMODULE” is compliant with IEEE 802.15.4 (2.4GHz band). The products include active tags, the base stations, and the relay stations. The sensor network is simply constructed with these products. Figure 1 shows an example of the system configurations. Active tags with omnidirectional pattern antennas and the base stations with the whip antennas are used in our experiments.

**3. Statistical Models of RSSI.** In wireless telecommunications, RSSI measurement data at each base station have large variations due to the influence of the radio environment. Often the Rice distribution (or Rician distribution) is used as a model of the PDF (probability density function) of the amplitude ( $X$ ) of the radio wave. Namely,

$$f_X(x) = \frac{x}{\sigma^2} e^{-\frac{x^2+A^2}{2\sigma^2}} I_0\left(\frac{x A}{\sigma^2}\right), \tag{1}$$

where  $I_n(x)$  is the  $n$ -th order modified Bessel function [13] of the first kind. Namely,

$$I_n(x) \equiv \frac{1}{\pi} \int_0^\pi e^{x \cos \theta} \cos n\theta d\theta. \tag{2}$$

Especially,  $n = 0$ , we have the relations

$$I_0(x) = \frac{1}{\pi} \int_0^\pi e^{\pm x \cos \theta} d\theta = \frac{1}{\pi} \int_0^\pi \cosh(x \cos \theta) d\theta = \frac{1}{\pi} \int_0^\pi \cosh(x \sin \theta) d\theta. \tag{3}$$

Also the power series expressions of  $I_n(x)$  are given by

$$I_n(x) = \left(\frac{x}{2}\right)^n \sum_{k=0}^\infty \frac{\left(\frac{x^2}{4}\right)^k}{k! \Gamma(n+k+1)} \tag{4}$$

and when specially  $n = 0$ , we have,

$$I_0(x) = \sum_{k=0}^\infty \frac{(x)^{2k}}{2^{2k} k! k!}. \tag{5}$$

Further, the PDF for the average power (or strength,  $Y = \frac{X^2}{2}$ ) of  $X$  is obtained by applying the relations

$$\frac{dx}{dy} = \frac{1}{\sqrt{2}} y^{-\frac{1}{2}}, \tag{6}$$

and

$$f_Y(y) = f_X(x) \left| \frac{dx}{dy} \right| = \frac{f_X(\sqrt{2y})}{\sqrt{2y}}. \tag{7}$$

Therefore, we have the PDF for the RSSI as follows

$$f_Y(y) = \frac{1}{\sigma^2} e^{-\frac{2y+A^2}{2\sigma^2}} I_0\left(\frac{\sqrt{2y} A}{\sigma^2}\right). \tag{8}$$

**3.1. Friis transmission formula – relation between RSSI and the distance.** In wireless communications, the RSSI attenuates by powers of the distance [14]. Therefore, in indoor environments, relations of the RSSI and the distance are unformulated by “power decay factor” due to near/far effect and “fading distribution”.

The formula originally proposed by Friis in 1946 [15], gives the relationship between the transmitted signal power  $P_t$  and receiver signal power  $P_r$  in a one-way, free-space radio link:

$$P_r = P_t \frac{G_t G_r \lambda^2}{(4\pi)^2 d^n}$$

where  $G_t$  and  $G_r$  are the transmitting and receiving antenna gains,  $\lambda$  is the wavelength,  $d$  is the distance between antennas, and  $n$  is the path loss exponent. This model is only assumed as the attenuation model that does not consider the reflection of radio waves. The correct values of antenna gains  $G_t$  and  $G_r$  are difficult to be obtained due to their large variations depending on circumstances of the nodes.

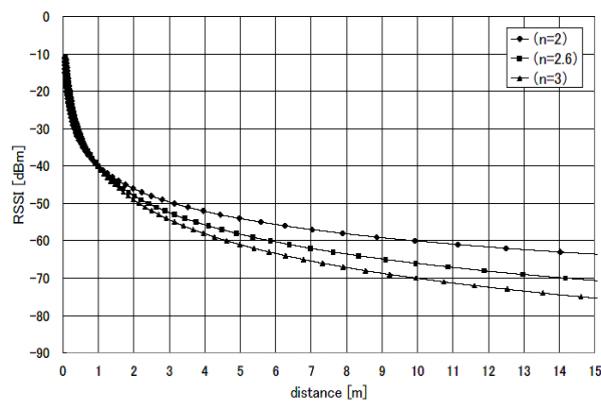


FIGURE 2. Friis equation curves

Figure 2 shows the Friis equation curves ( $G_t = 1$ ,  $G_r = 1$ ,  $P_t = 1$ ,  $\lambda = 0.1243$ ) with different values of  $n$ , that show a large change. Here, let us show the experimental

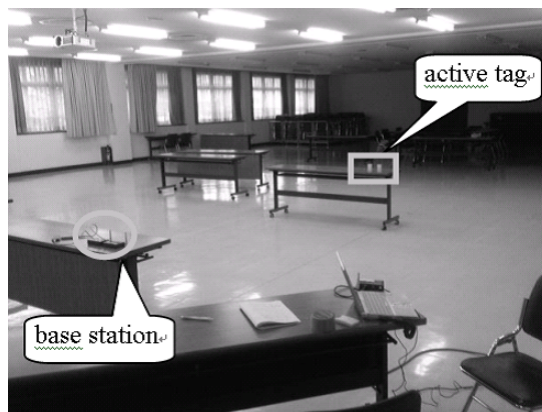


FIGURE 3. Measurement environment for testing the relation between RSSI and distance

results between the RSSIs and distances, where the measurement environment is shown in Figure 3. In experiments, two base stations are located at 1 meter high, and 1 [Hz] rate measurement data were collected for one minute at several points. Figure 4 shows

the RSSI measurement data at several points that are separately-placed (from 1 to 10 meters) from the base stations.

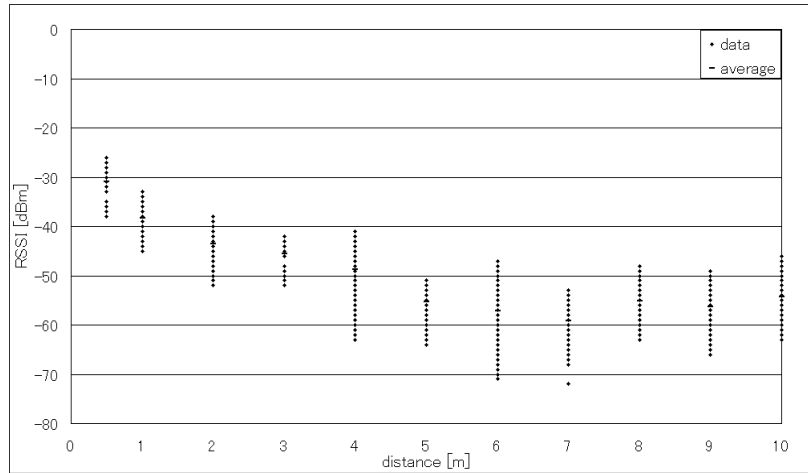


FIGURE 4. Measured RSSI values (15,000 measurements are plotted at each distance)

From Figure 4, we can observe that a large difference of values of the RSSI measured between each active tag and each base station exists. The distribution of values of the RSSI is changed by the installation environment and the individual differences in each base station. Therefore, it is important to consider the radio propagation model of the RSSI.

**4. ML Estimation Based on the Rice Distribution.** The PDF of the RSSI is given in (8). Then we assume from the Friis formula:

$$A = ad^{-b} \tag{9}$$

$$\sigma^2 = \alpha d^{-\beta} \tag{10}$$

where  $d$  is the distance between the transmitter (a tag) and receiver (a node).  $a$  and  $\alpha$  are intensities and  $b$  and  $\beta$  are attenuations. Substituting (9) and (10) into (8), we have a statistical model of RSSI, which is called the R-model hereafter.

$$f_Y(y) = \frac{1}{\alpha d^{-\beta}} e^{-\frac{2y_k + a^2 d^{-2b}}{2\alpha d^{-\beta}}} I_0 \left( \frac{\sqrt{2y_k} a d^{-b}}{\alpha d^{-\beta}} \right). \tag{11}$$

Now let us obtain the ML estimates of the unknown vector  $\theta \equiv [a, b, \alpha, \beta]^T$  based on the measurements of distances and RSSIs  $\{d_k, y_k; k = 1, 2, \dots, n\}$ . Then the likelihood function  $L_R(\theta)$  and the log-likelihood function  $l_R(\theta)$  are respectively obtained by

$$L_R(\theta) = \prod_{k=1}^n \frac{1}{\alpha d_k^{-\beta}} e^{-\frac{2y_k + a^2 d_k^{-2b}}{2\alpha d_k^{-\beta}}} I_0 \left( \frac{\sqrt{2y_k} a d_k^{-b}}{\alpha d_k^{-\beta}} \right), \tag{12}$$

and

$$\begin{aligned} l_R(\theta) &= \ln L(\theta) \\ &= \sum_{k=1}^n \left[ -\ln \alpha + \beta \ln d_k - \frac{2y_k + a^2 d_k^{-2b}}{2\alpha d_k^{-\beta}} + \ln I_0 \left( \frac{\sqrt{2y_k} a d_k^{-b}}{\alpha d_k^{-\beta}} \right) \right]. \end{aligned} \tag{13}$$

4.1. **ML estimates of  $\mathbf{a}, \mathbf{b}, \alpha, \beta$ .** Here we derive to obtain the ML estimates of the unknown vector  $\theta \equiv [a, b, \alpha, \beta]^T$  in (13). Applying the differential rule to the Modified Bessel function as follows:

$$\begin{aligned} \frac{d}{dx} \ln I_0(Fx) &= \frac{\frac{d}{dx} I_0(Fx)}{I_0(Fx)} \\ &= \frac{I_1(Fx)}{I_0(Fx)} F, \end{aligned} \tag{14}$$

then differentiation of (13) with respect to  $a, b, \alpha, \beta$  yields

$$\frac{\partial l_R(\theta)}{\partial a} = \sum_{k=1}^n \left\{ -\frac{a}{\alpha} d_k^{-2b+\beta} + \frac{I_1\left(\frac{\sqrt{2y_k a d_k^{-b}}}{\alpha d_k^{-\beta}}\right) \sqrt{2y_k} d_k^{-b+\beta}}{I_0\left(\frac{\sqrt{2y_k a d_k^{-b}}}{\alpha d_k^{-\beta}}\right) \alpha} \right\} = 0, \tag{15}$$

$$\frac{\partial l_R(\theta)}{\partial b} = \sum_{k=1}^n \left\{ \frac{a^2}{\alpha} d_k^{-2b+\beta} \ln d_k - \frac{I_1\left(\frac{\sqrt{2y_k a d_k^{-b}}}{\alpha d_k^{-\beta}}\right) a}{I_0\left(\frac{\sqrt{2y_k a d_k^{-b}}}{\alpha d_k^{-\beta}}\right) \alpha} \sqrt{2y_k} d_k^{-b+\beta} \ln d_k \right\} = 0, \tag{16}$$

$$\frac{\partial l_R(\theta)}{\partial \alpha} = \sum_{k=1}^n \left\{ -\frac{1}{\alpha} + \frac{2y_k + a^2 d_k^{-2b}}{2d_k^{-\beta} \alpha^2} - \frac{I_1\left(\frac{\sqrt{2y_k a d_k^{-b}}}{\alpha d_k^{-\beta}}\right) \sqrt{2y_k} a d_k^{-b+\beta}}{I_0\left(\frac{\sqrt{2y_k a d_k^{-b}}}{\alpha d_k^{-\beta}}\right) \alpha^2} \right\} = 0, \tag{17}$$

$$\frac{\partial l_R(\theta)}{\partial \beta} = \sum_{k=1}^n \left\{ \ln d_k - d_k^\beta \ln d_k \left( \frac{2y_k + a^2 d_k^{-2b}}{2\alpha} \right) + \frac{I_1\left(\frac{\sqrt{2y_k a d_k^{-b}}}{\alpha d_k^{-\beta}}\right) \sqrt{2y_k} a d_k^{-b+\beta}}{I_0\left(\frac{\sqrt{2y_k a d_k^{-b}}}{\alpha d_k^{-\beta}}\right) \alpha} \ln d_k \right\} = 0. \tag{18}$$

Then we can obtain the ML estimates for solving simultaneously four equations in (15)-(18).

**ML estimates of relative locations**

Once we get the model parameters in the log-likelihood function in (13), then inversely we can obtain the location  $(x_u, y_u, z_u)$  of the tag by obtaining the RSSI data  $\{y_k, k = 1, \dots, n_s\}$  for the receivers  $k = 1, \dots, n_s$ , whose locations  $(x_{r_k}, y_{r_k}, z_{r_k}), k = 1, \dots, n_s$  are known. The log-likelihood function of the tag's location is given by

$$l_R(x_u, y_u, z_u) = \sum_{k=1}^{n_s} \left[ -\ln \alpha + \beta \ln d_k - \frac{2y_k + a^2 d_k^{-2b}}{2\alpha d_k^{-\beta}} + \ln I_0\left(\frac{\sqrt{2y_k a d_k^{-b}}}{\alpha d_k^{-\beta}}\right) \right], \tag{19}$$

where

$$d_k \equiv \sqrt{(x_{r_k} - x_u)^2 + (y_{r_k} - y_u)^2 + (z_{r_k} - z_u)^2}. \tag{20}$$

The derivative of each term in (19) is evaluated as follows.

The derivative of the first term in (19):

$$\frac{\partial(-\ln \alpha)}{\partial x_u} = 0. \tag{21}$$

The derivative of the second term in (19):

$$\frac{\partial}{\partial x_u} (\beta \ln d_k) = \beta \frac{\frac{\partial}{\partial x_u} \{d_k\}}{d_k} = \frac{-\beta(x_{r_k} - x_u)}{(x_{r_k} - x_u)^2 + (y_{r_k} - y_u)^2 + (z_{r_k} - z_u)^2}. \tag{22}$$

The derivative of the third term in (19):

$$\begin{aligned}
 & \frac{\partial}{\partial x_u} \left( -\frac{2y_k + a^2 d_k^{-2b}}{2\alpha d_k^{-\beta}} \right) \\
 &= \frac{\partial}{\partial x_u} \left( -\frac{y_k}{\alpha} d_k^\beta - \frac{a^2}{2\alpha} d_k^{-2b+\beta} \right) \\
 &= -\frac{y_k}{\alpha} \frac{\beta}{2} [(x_{r_k} - x_u)^2 + (y_{r_k} - y_u)^2 + (z_{r_k} - z_u)^2]^{\frac{\beta}{2}-1} 2(x_{r_k} - x_u)(-1) \\
 &\quad - \frac{a^2}{2\alpha} \left( -b + \frac{\beta}{2} \right) [(x_{r_k} - x_u)^2 + (y_{r_k} - y_u)^2 + (z_{r_k} - z_u)^2]^{-b+\frac{\beta}{2}-1} 2(x_{r_k} - x_u)(-1) \\
 &= \frac{y_k \beta}{\alpha} (x_{r_k} - x_u) [(x_{r_k} - x_u)^2 + (y_{r_k} - y_u)^2 + (z_{r_k} - z_u)^2]^{\frac{\beta}{2}-1} \\
 &\quad + \frac{a^2}{\alpha} \left( -b + \frac{\beta}{2} \right) (x_{r_k} - x_u) [(x_{r_k} - x_u)^2 + (y_{r_k} - y_u)^2 + (z_{r_k} - z_u)^2]^{-b+\frac{\beta}{2}-1} \quad (23)
 \end{aligned}$$

The derivative of the fourth term in (19):

$$\begin{aligned}
 & \frac{\partial}{\partial x_u} \left\{ \ln I_0 \left( \frac{\sqrt{2y_k a d_k^{-b}}}{\alpha d_k^{-\beta}} \right) \right\} \\
 &= \frac{I_1 \left( \frac{\sqrt{2y_k a d_k^{-b}}}{\alpha d_k^{-\beta}} \right)}{I_0 \left( \frac{\sqrt{2y_k a d_k^{-b}}}{\alpha d_k^{-\beta}} \right)} \frac{\partial}{\partial x_u} \left\{ \frac{\sqrt{2y_k a d_k^{-b+\beta}}}{\alpha} \right\} \\
 &= \frac{I_1 \left( \frac{\sqrt{2y_k a d_k^{-b}}}{\alpha d_k^{-\beta}} \right)}{I_0 \left( \frac{\sqrt{2y_k a d_k^{-b}}}{\alpha d_k^{-\beta}} \right)} \frac{a\sqrt{2y_k} - b + \beta}{\alpha} \\
 &\quad \times [(x_{r_k} - x_u)^2 + (y_{r_k} - y_u)^2 + (z_{r_k} - z_u)^2]^{\frac{-b+\beta}{2}-1} 2(x_{r_k} - x_u)(-1) \\
 &= -\frac{I_1 \left( \frac{\sqrt{2y_k a d_k^{-b}}}{\alpha d_k^{-\beta}} \right)}{I_0 \left( \frac{\sqrt{2y_k a d_k^{-b}}}{\alpha d_k^{-\beta}} \right)} \frac{a\sqrt{2y_k}}{\alpha} (-b + \beta)(x_{r_k} - x_u) \\
 &\quad \times [(x_{r_k} - x_u)^2 + (y_{r_k} - y_u)^2 + (z_{r_k} - z_u)^2]^{\frac{-b+\beta}{2}-1}. \quad (24)
 \end{aligned}$$

Therefore, we finally have the relation

$$\begin{aligned}
 \frac{\partial l(x_u, y_u, z_u)}{\partial x_u} &= \sum_{k=1}^{n_s} \left\{ \frac{-\beta(x_{r_k} - x_u)}{(x_{r_k} - x_u)^2 + (y_{r_k} - y_u)^2 + (z_{r_k} - z_u)^2} \right. \\
 &\quad + \frac{y_k \beta}{\alpha} (x_{r_k} - x_u) [(x_{r_k} - x_u)^2 + (y_{r_k} - y_u)^2 + (z_{r_k} - z_u)^2]^{\frac{\beta}{2}-1} \\
 &\quad + \frac{a^2}{\alpha} \left( -b + \frac{\beta}{2} \right) (x_{r_k} - x_u) [(x_{r_k} - x_u)^2 + (y_{r_k} - y_u)^2 + (z_{r_k} - z_u)^2]^{-b+\frac{\beta}{2}-1} \\
 &\quad - \frac{I_1 \left( \frac{\sqrt{2y_k a d_k^{-b}}}{\alpha d_k^{-\beta}} \right)}{I_0 \left( \frac{\sqrt{2y_k a d_k^{-b}}}{\alpha d_k^{-\beta}} \right)} \frac{a\sqrt{2y_k}}{\alpha} (-b + \beta)(x_{r_k} - x_u) \\
 &\quad \left. \times [(x_{r_k} - x_u)^2 + (y_{r_k} - y_u)^2 + (z_{r_k} - z_u)^2]^{\frac{-b+\beta}{2}-1} \right\} = 0. \quad (25)
 \end{aligned}$$

In the similar computation, we have

$$\begin{aligned} \frac{\partial l_R(x_u, y_u, z_u)}{\partial y_u} &= \sum_{k=1}^{n_s} \left\{ \frac{-\beta(y_{r_k} - y_u)}{(x_{r_k} - x_u)^2 + (y_{r_k} - y_u)^2 + (z_{r_k} - z_u)^2} \right. \\ &\quad + \frac{y_k \beta}{\alpha} (y_{r_k} - y_u) [(x_{r_k} - x_u)^2 + (y_{r_k} - y_u)^2 + (z_{r_k} - z_u)^2]^{\frac{\beta}{2}-1} \\ &\quad + \frac{a^2}{\alpha} \left(-b + \frac{\beta}{2}\right) (y_{r_k} - y_u) [(x_{r_k} - x_u)^2 + (y_{r_k} - y_u)^2 + (z_{r_k} - z_u)^2]^{-b+\frac{\beta}{2}-1} \\ &\quad - \frac{I_1\left(\frac{\sqrt{2y_k a d_k^{-b}}}{\alpha d_k^{-\beta}}\right)}{I_0\left(\frac{\sqrt{2y_k a d_k^{-b}}}{\alpha d_k^{-\beta}}\right)} \frac{a\sqrt{2y_k}}{\alpha} (-b + \beta)(y_{r_k} - y_u) \\ &\quad \left. \times [(x_{r_k} - x_u)^2 + (y_{r_k} - y_u)^2 + (z_{r_k} - z_u)^2]^{-\frac{b+\beta}{2}-1} \right\} = 0 \end{aligned} \tag{26}$$

and

$$\begin{aligned} \frac{\partial l_R(x_u, y_u, z_u)}{\partial z_u} &= \sum_{k=1}^{n_s} \left\{ \frac{-\beta(z_{r_k} - z_u)}{(x_{r_k} - x_u)^2 + (y_{r_k} - y_u)^2 + (z_{r_k} - z_u)^2} \right. \\ &\quad + \frac{y_k \beta}{\alpha} (z_{r_k} - z_u) [(x_{r_k} - x_u)^2 + (y_{r_k} - y_u)^2 + (z_{r_k} - z_u)^2]^{\frac{\beta}{2}-1} \\ &\quad + \frac{a^2}{\alpha} \left(-b + \frac{\beta}{2}\right) (z_{r_k} - z_u) [(x_{r_k} - x_u)^2 + (y_{r_k} - y_u)^2 + (z_{r_k} - z_u)^2]^{-b+\frac{\beta}{2}-1} \\ &\quad - \frac{I_1\left(\frac{\sqrt{2y_k a d_k^{-b}}}{\alpha d_k^{-\beta}}\right)}{I_0\left(\frac{\sqrt{2y_k a d_k^{-b}}}{\alpha d_k^{-\beta}}\right)} \frac{a\sqrt{2y_k}}{\alpha} (-b + \beta)(z_{r_k} - z_u) \\ &\quad \left. \times [(x_{r_k} - x_u)^2 + (y_{r_k} - y_u)^2 + (z_{r_k} - z_u)^2]^{-\frac{b+\beta}{2}-1} \right\} = 0 \end{aligned} \tag{27}$$

**4.2. A special model I ( $a = 0 = A$ ) – (S1-model).** Here we assume  $a \equiv 0$  (then  $A = 0$ ) in (9), then the PDF in (8) is the exponential distribution, which corresponds to the strength (average power) of the random variable of the Rayleigh distribution. Namely, with (10), the PDF in (8) becomes

$$\begin{aligned} f_Y(y) &= \frac{1}{\sigma^2} \exp\left\{-\frac{y}{\sigma^2}\right\} \\ &= \frac{1}{\alpha d_k^{-\beta}} \exp\left\{-\frac{y}{\alpha d_k^{-\beta}}\right\} \end{aligned} \tag{28}$$

Then the log-likelihood function is given by

$$\begin{aligned} l_1(\theta) &\equiv \ln \left[ \prod_{k=1}^n \frac{1}{\alpha d_k^{-\beta}} e^{-\frac{2y_k}{2\alpha d_k^{-\beta}}} I_0(0) \right] \\ &= \sum_{k=1}^n \left[ -\ln \alpha + \beta \ln d_k - \frac{y_k}{\alpha d_k^{-\beta}} \right], \end{aligned} \tag{29}$$

where we use the relation  $I_0(0) = 1$ .



4.3. **ML estimates of  $\alpha$ ,  $\beta$  in (28).** For the log-likelihood function (29), we also obtain the ML estimates of  $\alpha$ ,  $\beta$  in the S1 model. Taking the partial derivatives of (29) by  $\alpha$  and  $\beta$ , we have

$$\frac{\partial l_1(\theta)}{\partial \alpha} = \sum_{k=1}^n \left[ -\frac{1}{\alpha} + \frac{y_k}{\alpha^2 d_k^{-\beta}} \right] = 0 \quad (30)$$

$$\frac{\partial l_1(\theta)}{\partial \beta} = \sum_{k=1}^n \left[ \ln d_k - \frac{y_k}{\alpha} d_k^\beta \ln d_k \right] = 0 \quad (31)$$

By solving simultaneously the above two equations in (30) and (31), we can obtain ML estimates of  $\alpha$ ,  $\beta$ , in case of  $A = 0$ .

4.4. **Gamma distribution – (the G-model).** The measurement data of RSSI are usually provided by the average values  $\bar{Y}$  of  $\{Y_k, k = 1, \dots, m\}$ :

$$\bar{Y} = \frac{1}{m} \sum_{k=1}^m Y_k,$$

where we assume each measurement is statistically independent each other. Then the PDF of  $\bar{Y}$  can be obtained as the following gamma distribution

$$p_{\bar{Y}}(\bar{y}) = \frac{1}{\left(\frac{\sigma^2}{m}\right)^m \Gamma(m)} \bar{y}^{m-1} \exp \left\{ -\frac{\bar{y}}{\frac{\sigma^2}{m}} \right\}. \quad (32)$$

where  $\Gamma(m)$  is the gamma function defined by

$$\Gamma(m) \equiv \int_0^\infty z^{m-1} e^{-z} dz \quad (33)$$

#### ML estimation for parameters in the gamma distribution

Combining (10) and (32), the likelihood function of the  $\alpha$  and  $\beta$  is provided by

$$L_\gamma(\alpha, \beta) = \prod_{i=1}^n p_{\bar{Y}_i}(\bar{y}_i) = \prod_{i=1}^n \frac{1}{\left(\frac{\sigma_i^2}{m}\right)^m \Gamma(m)} \bar{y}_i^{m-1} e^{-\frac{m\bar{y}_i}{\sigma_i^2}} \quad (34)$$

Then, the log likelihood function  $l(\alpha, \beta)$  is also given by

$$\begin{aligned} l_\gamma(\alpha, \beta) &= \ln L_\gamma(\alpha, \beta) \\ &= \ln \left[ \prod_{i=1}^n \frac{1}{\left(\frac{\sigma_i^2}{m}\right)^m \Gamma(m)} \bar{y}_i^{m-1} e^{-\frac{m\bar{y}_i}{\sigma_i^2}} \right] \end{aligned} \quad (35)$$

where  $\sigma_i^2 = \alpha d_i^{-\beta}$ . Therefore, the log likelihood function given by the observation  $\{\bar{y}_1, \bar{y}_2, \dots, \bar{y}_n\}$  in each distance  $d_i$  from the above equation as follows:

$$l_\gamma(\alpha, \beta) = \sum_{i=1}^n \left[ -m \ln \left( \frac{\alpha}{m d_i^\beta} \right) - \ln \Gamma(m) + (m-1) \ln \bar{y}_i - \frac{m \bar{y}_i d_i^\beta}{\alpha} \right] \quad (36)$$

Then we have the following relations:

$$\frac{\partial l_\gamma}{\partial \alpha} = \sum_{i=1}^n \left[ -\frac{m}{\alpha} + \frac{m\bar{y}_i d_i^\beta}{\alpha^2} \right] = 0 \tag{37}$$

$$\frac{\partial l_\gamma}{\partial \beta} = \sum_{i=1}^n m \ln d_i - \frac{m\bar{y}_i d_i^\beta}{\alpha} \ln d_i = 0. \tag{38}$$

The solutions of the above nonlinear simultaneous equations are derived. From (37),

$$\frac{1}{\alpha} \left[ \sum_{i=1}^n (-m) + \frac{1}{\alpha} \sum_{i=1}^n m\bar{y}_i d_i^\beta \right] = 0.$$

If  $\alpha \neq 0$ ,

$$\sum_{i=1}^n (-m) + \frac{1}{\alpha} \sum_{i=1}^n m\bar{y}_i d_i^\beta = 0,$$

or

$$\alpha = \frac{1}{n} \sum_{i=1}^n \bar{y}_i d_i^\beta. \tag{39}$$

Now, we define  $\eta \equiv e^\beta$  and remark the following relation:

$$d_i^\beta = e^{\beta \ln d_i} = \eta^{\ln d_i}. \tag{40}$$

Then, from (38) and (40), we have

$$n \sum_{i=1}^n \bar{y}_i \eta^{\ln d_i} \ln d_i - \left( \sum_{i=1}^n \ln d_i \right) \sum_{k=1}^n \bar{y}_k \eta^{\ln d_k} = 0. \tag{41}$$

Therefore,  $\alpha$  and  $\beta$  can be estimated by solving the nonlinear equation of  $\eta$  in (41). Then we can obtain

$$\begin{aligned} \hat{\beta} &= \ln \hat{\eta}, \\ \hat{\alpha} &= \frac{1}{n} \sum_{i=1}^n \frac{\bar{y}_i r_i}{(d_i)^{\hat{\beta}}}. \end{aligned} \tag{42}$$

**Location estimation**

The node position  $[x_u \ y_u \ z_u]^T$  is estimated by the distance measured from the multiple base stations  $[x_i \ y_i \ z_i]^T$ ; ( $i = 1, 2, \dots, n_s$ ). The distance between the node and the base station  $i$  is expressed by

$$d_i = \sqrt{(x_i - x_u)^2 + (y_i - y_u)^2 + (z_i - z_u)^2} \tag{43}$$

From (32), the log-likelihood function of the unknown position  $[x_u \ y_u \ z_u]^T$  is provided by

$$L_\gamma(x_u, y_u, z_u) = \prod_{i=1}^{n_s} p_{Y_i}(\bar{y}_i) \Big|_{\sigma^2 = \alpha[(x_i - x_u)^2 + (y_i - y_u)^2 + (z_i - z_u)^2]^{-\frac{\beta}{2}}} \tag{44}$$

The node position  $[x_u \ y_u \ z_u]^T$  is estimated by the ML method. Then, the log likelihood function  $l(x_u, y_u, z_u)$  is also given by

$$l_\gamma(x_u, y_u, z_u) = \ln L_\gamma(x_u, y_u, z_u) \tag{45}$$

namely,

$$\begin{aligned}
 l_\gamma(x_u, y_u, z_u) &= \sum_{i=1}^{n_s} \ln P_{\bar{Y}_i}(\bar{y}_i) \Big|_\theta \\
 &= \sum_{i=1}^{n_s} \ln \frac{1}{\left(\frac{\theta}{m}\right)^m \Gamma(m)} \bar{y}_i^{m-1} e^{-\frac{m\bar{r}_i}{\sigma^2}} \Big|_{\sigma^2} \\
 &= \sum_{i=1}^{n_s} \left( -m \ln \left( \frac{\sigma^2}{m} \right) - \ln \Gamma(m) + (m-1) \ln \bar{y}_i - \frac{m\bar{y}_i}{\sigma^2} \right) \Big|_{\sigma^2} \\
 &= \sum_{i=1}^{n_s} \left\{ -\frac{m\beta}{2} \ln [(x_i - x_u)^2 + (y_i - y_u)^2 + (z_i - z_u)^2] \right. \\
 &\quad \left. - m\bar{r}_i \left[ \alpha^{-1} ((x_i - x_u)^2 + (y_i - y_u)^2 + (z_i - z_u)^2)^{\frac{\beta}{2}} \right] \right. \\
 &\quad \left. + (-m) \ln \alpha + \text{const.} \right\} \tag{46}
 \end{aligned}$$

The maximum likelihood estimate of  $[x_u \ y_u \ z_u]^T$  is obtained by maximizing (46); therefore,  $(x_u, y_u, z_u)$  is derived by nonlinear simultaneous equations:

$$\begin{aligned}
 \frac{\partial l_\gamma}{\partial x_u} &= \sum_{i=1}^n \left\{ \frac{-m\beta(x_i - x_u)}{(x_i - x_u)^2 + (y_i - y_u)^2 + (z_i - z_u)^2} \right. \\
 &\quad \left. + \frac{2m\bar{y}_i(x_i - x_u)}{\alpha [(x_i - v_u)^2 + (y_i - y_u)^2 + (z_i - z_u)^2]^{\frac{-\beta+2}{2}}} \right\} = 0 \\
 \frac{\partial l_\gamma}{\partial y_u} &= \sum_{i=1}^n \left\{ \frac{-m\beta(y_i - y_u)}{(x_i - x_u)^2 + (y_i - y_u)^2 + (z_i - z_u)^2} \right. \\
 &\quad \left. + \frac{2m\bar{r}_i(y_i - y_u)}{\alpha [(x_i - v_u)^2 + (y_i - y_u)^2 + (z_i - z_u)^2]^{\frac{\beta+2}{2}}} \right\} = 0 \\
 \frac{\partial l_\gamma}{\partial z_u} &= \sum_{i=1}^n \left\{ \frac{-m\beta(z_i - z_u)}{(x_i - x_u)^2 + (y_i - y_u)^2 + (z_i - z_u)^2} \right. \\
 &\quad \left. + \frac{2m\bar{y}_i(z_i - z_u)}{\alpha [(x_i - v_u)^2 + (y_i - y_u)^2 + (z_i - z_u)^2]^{\frac{\beta+2}{2}}} \right\} = 0 \tag{47}
 \end{aligned}$$

**4.5. A special model II ( $b = \beta$ ) – (the S2 model).** Also if we assume the attenuations  $b$  and  $\beta$  are the same ( $b = \beta$ ) in the R-model in (11), then we have the log-likelihood function as follows.

$$l_2(\theta) \equiv \sum_{k=1}^n \left[ -\ln \alpha + \beta \ln d_k - \frac{2y_k + a^2 d_k^{-2\beta}}{2\alpha d_k^{-\beta}} + \ln I_0 \left( \frac{a\sqrt{2y_k}}{\alpha} \right) \right]. \tag{48}$$

**ML estimates of  $a, \alpha, \beta = b$**

Similarly for the log-likelihood function (48), we can obtain the ML estimates of  $a, \alpha, \beta (= b)$ . Namely Taking the partial derivatives of (48) with respect to  $a, \alpha$  and  $\beta$ , we have

$$\frac{\partial l_2(\theta)}{\partial a} = \sum_{k=1}^n \left[ -\frac{a}{\alpha} d_k^{-\beta} + \frac{I_1 \left( \frac{a\sqrt{2y_k}}{\alpha} \right)}{I_0 \left( \frac{a\sqrt{2y_k}}{\alpha} \right)} \frac{\sqrt{2y_k}}{\alpha} \right] = 0 \tag{49}$$

$$\frac{\partial l_2(\theta)}{\partial \alpha} = \sum_{k=1}^n \left[ -\frac{1}{\alpha} + \frac{y_k}{\alpha^2 d_k^{-\beta}} - \frac{a^2}{2\alpha^2} d_k^{-\beta} - \frac{I_1\left(\frac{a\sqrt{2y_k}}{\alpha}\right)}{I_0\left(\frac{a\sqrt{2y_k}}{\alpha}\right)} \frac{a\sqrt{2y_k}}{\alpha^2} \right] = 0 \quad (50)$$

$$\frac{\partial l_2(\theta)}{\partial \beta} = \sum_{k=1}^n \left[ \ln d_k + \left(\frac{\ln d_k}{\alpha}\right) \left(-y_k d_k^\beta + \frac{a^2}{2} d_k^{-\beta}\right) \right] = 0 \quad (51)$$

By solving three equations in (49)-(51), we have ML estimates of  $a$ ,  $\alpha$ ,  $\beta$  in case of assuming  $\beta = b$ .

**4.6. Fitness of models.** Four models of RSSI, namely, the R-model in Section 4, the S1-model in Section 4.2, the G-model in Section 4.4, and the S2-models in Section 4.5, have been presented. The best model of the RSSI among these four models is chosen by minimizing the famous AIC (Akaike's information criterion) [11, 12] as follows:

$$\text{AIC} \equiv (-2) \times \ln(\text{maximum likelihood}) + 2 \times (\text{No. of parameters in the model}). \quad (52)$$

**5. Experimental Results.** The experiments of estimating the parameters and location were carried out in the same environment shown in Figure 3. The parameters of the nodes (tag) are shown in Table 1.

TABLE 1. Experimental condition of active tag

Condition	parameter
Frequency	2405 [MHz]
Power ( $P_t$ )	1 [mW]
Sampling interval	1 [sec]

**5.1. Estimating the parameters.** We show the estimation results of  $a$ ,  $b$ ,  $\alpha$  and  $\beta$  using the RSSI data with 1-18 meters. The proposed models were evaluated for using about 1,000 data in each distance. Table 2 shows the results of ML estimation for parameters and AIC, where the data set of G-model is  $m = 8$ .

TABLE 2. Estimation results of  $a, b, \alpha, \beta$  and AIC

Models	$\hat{a}$	$\hat{b}$	$\hat{\alpha}$	$\hat{\beta}$	AIC
G-model	–	–	0.00008	2.315215	–81291.955170
S1-model	–	–	0.00001	1.228144	–172159.258796
S2-model	0.000034	–	0.000089	2.356846	–165752.990581
R-model	0.000018	1.664221	0.000091	2.365100	–165670.485998

We can see that  $\alpha$ ,  $\beta$  of G-model, S1-model and S2-model produced the almost same results. Also, S1-model is best model from AIC results, but there is not much difference among these four models.

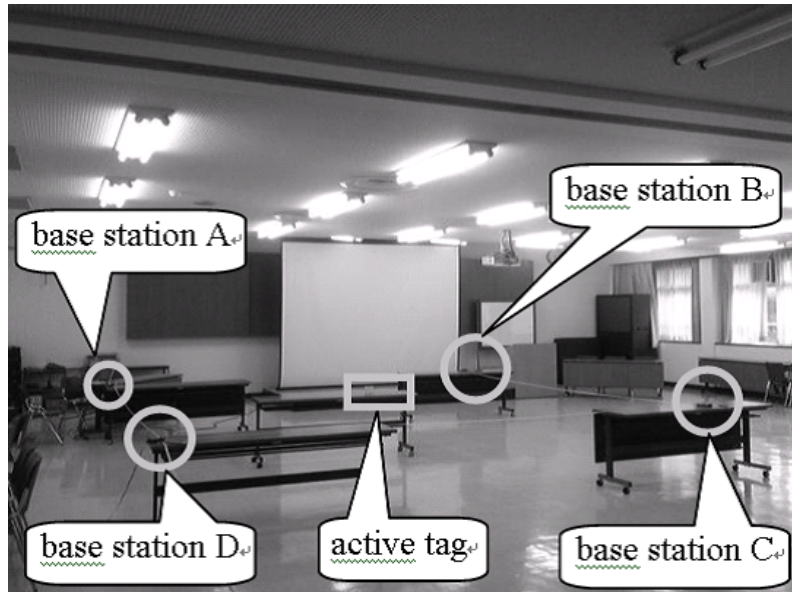


FIGURE 5. Experimental environment

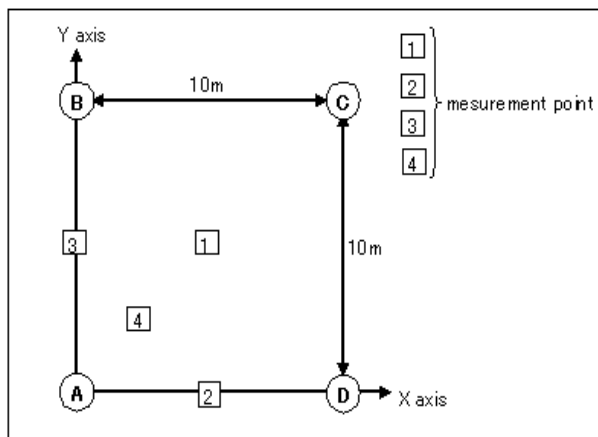


FIGURE 6. Measurement points in 10 [m] square shape

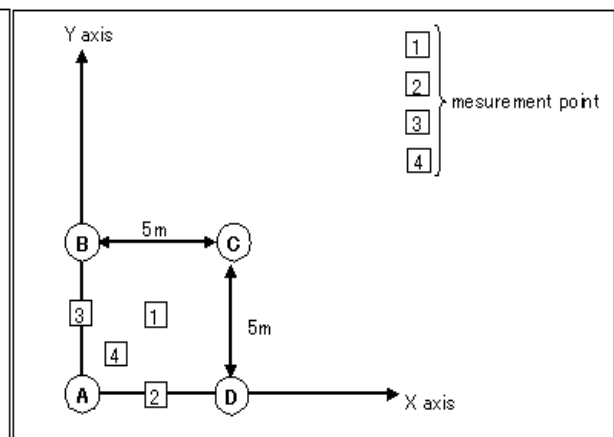


FIGURE 7. Measurement points in 5 [m] square shape

TABLE 3. Experimental condition of equipments

Device	number	Notes
Active tag	1	Height: 1.0 [m]
Base station	4	Height: 1.0 [m]

5.2. **Location results.** Next, we experimented on the location estimation by using the estimation results of  $a$ ,  $b$ ,  $\alpha$  and  $\beta$  (Table 2). As shown in Figure 5, four base stations were located in a 10 [m] or 5 [m] square shape. Therefore, the evaluation data are different from estimating the parameters. Figures 6 and 7 show the coordinates of the base stations and tags.

The heights of all the objects, namely the base stations and tags were fixed at 1.0 [m] from the floor. Therefore, in this experiment, the location estimation was implemented in the horizontal (2D) plane. In the experiments, the location of tags plotted by a symbol of square in Figure 6 were estimated twice by using two independent datasets. The location

of tags plotted by a symbol of square in Figures 6 and 7. Each dataset was RSSI data collected at 1 [Hz] rate for about 400 seconds by the base stations. In addition, experiments of Figure 6 were estimated twice by using two independent datasets. We compared the difference between the position calculated and the true position, and evaluated by calculating the average and variance of each of the X and Y axis.

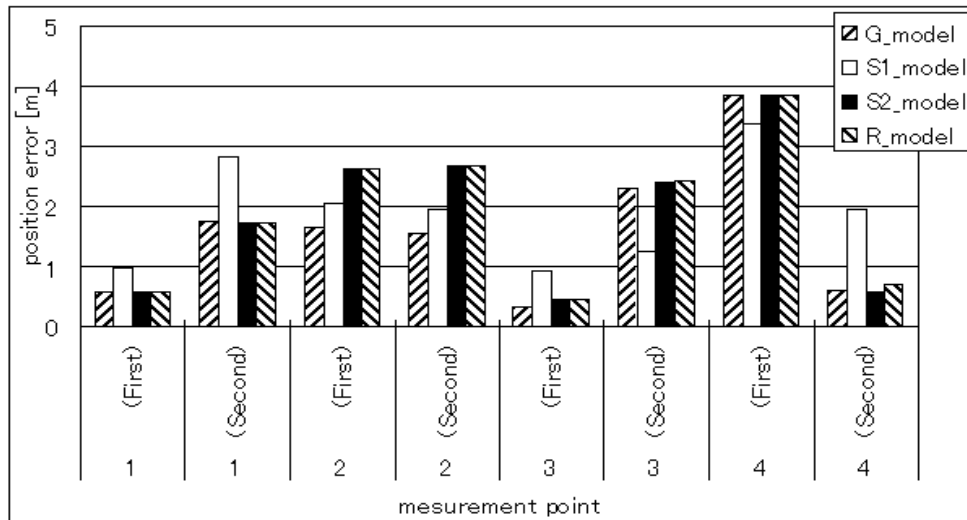


FIGURE 8. The position errors in 10 [m] square shape

Figure 8 shows the results of position errors applying ML estimation based on the proposed four models for the measurement points in the 10 [m] square shape shown in Figure 6. It can be seen that estimated position errors based on each model are about 0.5 to 4 meters. Especially, the G-model provided good accuracy in almost measurement points.

Table 4 shows the results of the averages of estimated positions and the variances of positioning errors, for each axis in Figure 8. We can see from Table 4 that the S2-model and the R-model achieved almost equivalent good performance. On the other hand in case of the S1-model and G-model, these values of the variance are large compared with the S2-model and the R-model.

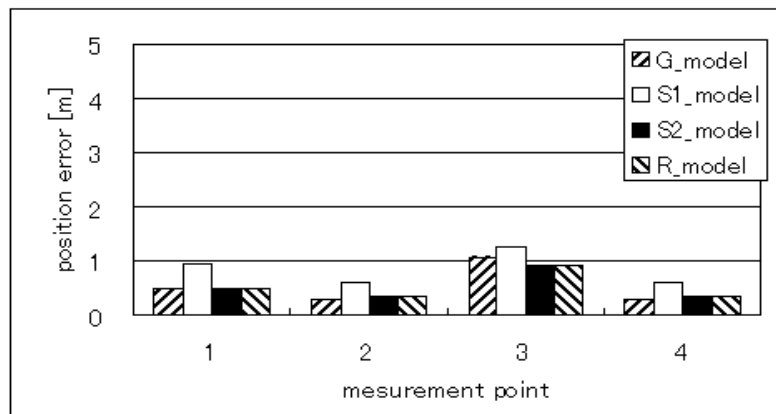


FIGURE 9. The position errors in the 5 [m] square shape

Figure 9 shows the results of positioning errors applying these four models in the 5 [m] square shape. We can see from Figure 9, the each models are calculated error of about 1 meter.

TABLE 4. Positioning results in the 10 [m] square shape

data	1(First)				1(Second)			
	X axis		Y axis		X axis		Y axis	
True	5 [m]		5 [m]		5 [m]		5 [m]	
	Average	Std. Dev.	Average	Std. Dev.	Average	Std. Dev.	Average	Std. Dev.
G-model	5.064	0.839	4.426	1.362	5.621	1.089	3.353	0.707
S1-model	5.372	2.579	4.103	3.042	6.191	1.693	2.432	1.004
S2-model	5.063	0.822	4.439	1.328	5.614	1.079	3.376	0.684
R-model	5.062	0.817	4.441	1.323	5.612	1.076	3.381	0.682
data	2(First)				2(Second)			
	X axis		Y axis		X axis		Y axis	
True	5 [m]		0 [m]		5 [m]		0 [m]	
	Average	Std. Dev.	Average	Std. Dev.	Average	Std. Dev.	Average	Std. Dev.
G-model	3.371	1.981	0.159	1.989	4.172	3.037	1.302	3.846
S1-model	2.957	2.929	-0.009	1.424	4.047	3.718	1.701	4.404
S2-model	2.670	2.358	1.194	2.432	4.126	2.493	2.523	3.634
R-model	2.666	2.357	1.196	2.438	4.128	2.491	2.528	3.625
data	3(First)				3(Second)			
	X axis		Y axis		X axis		Y axis	
True	0 [m]		5 [m]		0 [m]		5 [m]	
	Average	Std. Dev.	Average	Std. Dev.	Average	Std. Dev.	Average	Std. Dev.
G-model	0.333	2.405	5.045	1.060	2.288	0.823	5.177	0.468
S1-model	0.782	1.645	5.514	2.326	1.212	0.782	5.312	1.496
S2-model	0.436	2.075	5.000	0.842	2.401	0.748	5.182	0.478
R-model	0.433	2.078	4.999	0.837	2.409	0.746	5.181	0.476
data	4(First)				4(Second)			
	X axis		Y axis		X axis		Y axis	
True	2.5 [m]		2.5 [m]		2.5 [m]		2.5 [m]	
	Average	Std. Dev.	Average	Std. Dev.	Average	Std. Dev.	Average	Std. Dev.
G-model	5.215	1.425	5.204	1.160	2.887	0.586	2.963	1.260
S1-model	4.629	2.458	5.113	2.703	0.907	1.465	1.339	0.862
S2-model	5.250	1.446	5.194	1.131	2.876	0.615	2.929	1.369
R-model	5.251	1.443	5.194	1.127	2.797	0.597	3.130	1.167

TABLE 5. Positioning results in the 5 [m] square shape

data	1				2			
	X axis		Y axis		X axis		Y axis	
True	2.5 [m]		2.5 [m]		2.5 [m]		0 [m]	
	Average	Std. Dev.	Average	Std. Dev.	Average	Std. Dev.	Average	Std. Dev.
G-model	2.125	0.458	2.852	0.463	2.300	1.052	0.575	1.059
S1-model	1.746	1.079	3.092	0.993	2.077	1.262	0.470	1.053
S2-model	2.126	0.462	2.848	0.451	2.397	1.144	0.436	1.091
R-model	2.127	0.461	2.847	0.449	2.398	1.144	0.441	1.092
data	3				4			
	X axis		Y axis		X axis		Y axis	
True	0 [m]		2.5 [m]		1.25 [m]		1.25 [m]	
	Average	Std. Dev.	Average	Std. Dev.	Average	Std. Dev.	Average	Std. Dev.
G-model	0.791	0.790	1.758	0.710	1.438	1.050	2.037	1.029
S1-model	-0.662	0.275	1.402	0.811	0.833	1.021	2.063	1.357
S2-model	0.715	0.746	1.904	0.510	1.415	0.991	2.126	0.936
R-model	0.720	0.748	1.904	0.509	1.416	0.993	2.127	0.933

Table 5 shows the results of the average of estimated position errors, and the variance of position errors at each axis in Figure 9. Similarly, it can be seen that the S1-model and the R-model results are good performance regarding the variance. From Tables 4 and 5, the R-model is considered to increase the reliability of the positioning due to less variability when compared with other models.

**6. Conclusions.** In this paper, we considered positioning method by utilizing the models of radio propagation in sensor network. The models were identified from the Rice distribution using the maximum-likelihood method. We carried out experiments of the estimation of the model parameters and the location. In installation environment, the model of radio propagation was identified accurately, and the location estimation results show superior performance of ML method based on Rice distribution. Especially, the R-model applying the different parameter of attenuation coefficient provides better positioning accuracy. However, for the applications of positioning using RSSI, more stable positioning results are desired. In the future works, an accurate positioning estimation algorithm will be developed for practical use.

#### REFERENCES

- [1] Institute of Electrical and Electronics Engineers, *IEEE Std 802.15.4-2006, Wireless Medium Access Control (MAC) and Physical Layer (PHY) Specifications for Low-Rate Wireless Personal Area Networks (WPANs)*, 2006.
- [2] H. Niwa, K. Kodaka, Y. Sakamoto and S. Sugano, Indoor GPS receiver for mobile robot, *Proc. of International Symposium on GPS/GNSS*, vol.2, pp.511-516, 2008.
- [3] Japan Aerospace Exploration Agency, *Quasi-Zenith Satellite System Navigation Service Interface Specification for QZSS (IS-QZSS) V1.0*, 2008.
- [4] S. Hara, D. Zhao, K. Yanagihara, J. Taketsugu, K. Fukui, S. Fukunaga and K. Kitayama, Propagation characteristics of IEEE 802.15.4 radio signal and their application for location estimation, *Proc. of IEEE VTC*, 2005.
- [5] S. Capkun, M. Hamdi and J. Hubaux, GPS-free positioning in mobile Adhoc networks, *Proc. of the 34th HICSS*, pp.3481-3490, 2001.
- [6] A. Savvides, C. Han and M. B. Strivastava, Dynamic fine grained localization in AdHoc networks of sensors, *Proc. of ACM/IEEE MOBICOM*, 2001.
- [7] Y. Kubo, S. Fujioka, M. Nishiyama and S. Sugimoto, Nonlinear filtering methods for the INS/GPS in-motion alignment and navigation, *International Journal of Innovative Computing, Information and Control*, vol.2, no.5, pp.1137-1151, 2006.
- [8] M. Tanikawara, Y. Kubo and S. Sugimoto, Modeling of sensor error equations for GPS/INS hybrid systems, *International Journal of Innovative Computing, Information and Control*, vol.6, no.1, pp.127-138, 2010.
- [9] S. O. Rice, Mathematical analysis of random noise, *The Bell System Technical Journal*, vol.23, pp.282-332, 1944.
- [10] S. O. Rice, Mathematical analysis of random noise, *The Bell System Technical Journal*, vol.24, pp.46-156, 1945.
- [11] H. Akaike, A new look at the statistical model identification, *IEEE Trans. Automat. Contr.*, vol.19, pp.716-723, 1974.
- [12] G. Kitagawa, *Time-series Analysis*, Iwanami-Shoten, Tokyo, 2005 (in Japanese).
- [13] S. Okui, *Special Functions and Its Applications*, Morikita Shuppan, Tokyo, 1997 (in Japanese).
- [14] D. K. Barton and S. A. Leonov, *Radar Technology Encyclopedia*, Artech Print on Demand, 1997.
- [15] H. T. Friis, A note on a simple transmission formula, *Proc. of IRE and Wave and Electrons*, pp.254-256, 1946.